ISSN: 0975-766X
CODEN: IJPTFI
Available Online through
Research Article
www.ijptonline.com

EFFECTS OF RADIATION AND HEAT SOURCE ON DISSIPATIVE MHD FLOW OF WILLIAMSON NANOFLUID OVER A NONLINEAR VARIABLE THICKED SURFACE WITH MELTING HEAT TRANSFER

K. Suneetha[*], S. M. Ibrahim[†], G V Ramana Reddy[††]

[*]Research Scholar, Department of Mathematics, K. L University Vaddeswaram, Guntur(Dt), 502522, India.
[†]Department of Mathematics, GITAM University, Visakhapatnam, Andhra Pradesh- 530045., India.
[††]Department of Mathematics, K L University Vaddeswaram, Guntur(Dt), 502522, India.
Email: s.sunibabu@gmail.com

Received on: 15-08-2017 *Accepted on: 22-09-2017*

Abstract:

In this picture, we explored the effectiveness of magnetic nanoparticles and melting heat transfer in the stretched flow. Considered nonlinear nanofluid model consists of Brownian motion and thermophoresis mechanisms. Flow formulation is developed using rheological expressions of Williamson fluid. Thickness of nonlinear stretching surface is variable. Thermal radiation, viscous dissipation and heat source are also considered into account. Numerical solutions are displayed with help of graphs and tables. In addition, the systems of nonlinear ordinary differential equations (ODEs) are solved by using the Runge-Kutta-Fehlberg method (RKFM). We also validated the current results and found a satisfactory agreement. Impacts of various pertinent parameters on the non-dimensional velocity, temperature, concentration, skin friction, local Nusselt and local Sherwood numbers are analyzed in detail. It is anticipated that impact of melting heat transfer parameter on velocity and temperature is opposite.

Keywords: Williamson nanofluid; melting heat transfer; variable sheet thickness; MHD radiation.

Introduction

The study of nanofluids has attracted enormous interest from research because of its outstanding applications to electronics, communication, computing technologies, optical devices, lasers, high-power X-rays, material processing, scientific measurement, medicine and material synthesis. The word nanofluid was initiated by Choi [1]. He explained that the nanoparticles increases the thermal conductivity of base fluids and therefore substantially enhances the heat

transfer characteristics of the nanofluid. Later, Eastman et al. [2], Xie et al. [3] and Jana et al. [4] showed that higher thermal conductivity can be achieved in thermal systems utilizing nanofluids.

To elucidate the characteristics of pseudoplastic materials different models have been suggested like the Ellis model, Cross model, Carreau model and power law model however little consideration has been given to the Williamson liquid model. In 1929, Williamson [5] experimentally proposed a model for the description of flow of pseudoplastic fluids. The flow of Williamson fluid over a stretched surface model was analyzed by Nadeem et al. [6].

The exact solution for the flow due to stretching of flat surface was first obtained by Crane [7]. He was investigated the steady flow of an incompressible viscous fluid over an elastic sheet, where as the flow was caused by the stretching of the sheet in its own plane with a velocity varying linearly with the distance from a fixed point. The solution of the three-dimensional fluid motion caused by the stretching boundary was studied by Wang [8]. Andersson [9] has explained an exact solution of the flow of a viscoelastic fluid past a stretching sheet in the presence of a transverse magnetic field is considered. All the above studies are considered only for a linear stretching sheet, but it is true that not in all cases the stretching sheet is linear. It was first identified by Gupta and Gupta [10]. The study of heat transfer in a viscous fluid over a non-linearly stretching sheet with viscous dissipation was done by Vajravelu [11]. The flow of an incompressible viscous fluid over a non-linear stretching sheet in the presence of chemical reaction and magnetic field was investigated by Raptis and Perdiks [12]. Cortell [13] explained a numerical analysis for flow and heat transfer in a viscous fluid over a non-linear stretching sheet.

Magneto-fluid-dynamics or hydro-magnetics is a field of research which analyzes the dynamics of electricity conducting fluids such as plasmas, liquid metals and salt water. The term magnetohydrodynamics (MHD) is a combination of magneto (magnetic field), hydro (liquid) and dynamics (movement of particles). The magnetic field induced current flows in a dynamic fluid and creates forces on the fluid. Some important applications of radiative heat transfer include MHD accelerators, high temperature plasmas, power generation systems and cooling of nuclear reactors. Hayat et al. [14] studied the two dimensional MHD flow of Williamson nanofluid over a nonlinear variable thicked surface with melting heat transfer. Recently Mabood et al. [15] derived the effects of radiation on Williamson nanofluid flow over a heated surface in presence of magnetohydrodynamics. Numerous researchers [16 - 20] reported related studies for MHD and radiation effects. There may be an appreciable temperature difference between the surface and the ambient fluid in

many situations, this necessitates the consideration of temperature dependent heat sources or sinks which may exert strong influence on the heat transfer characteristics. Sumalatha and Shankar [21] studied the effects of radiation and heat source on a Casson fluid flow over a nonlinear stretching sheet. Radiation and non-uniform heat source effects on MHD viscoelastic boundary layer flow over a stretching sheet was studied by Nandeppanavar et al. [22]. Bhattacharyya [23] derived the effects of radiation and heat source on unsteady MHD boundary layer flow over a shrinking sheet in presence of suction and injection. Dissipation is the process of converting mechanical energy of downward-flowing water into thermal and acoustical energy. Various devices are designed in streambeds to reduce the kinetic energy of flowing waters, reducing their erosive potential on banks and river bottoms. Dessie and Kishan [24] presented the viscous dissipation and heat source effects on MHD heat transfer over stretching sheet embedded in porous medium with variable viscosity. The effects of viscous dissipation on MHD heat transfer nanofluid flow over an exponentially stretching sheet was discussed by Krishnamurthy et al. [25]. Sreenivasulu et al. [26] presented the importance of radiation and uniform heat source on MHD nanofluids past a nonlinear stretching sheet with viscous dissipation. Several previous authors such as Chamkha and Aly [27], Abel and Begum [28], Ibrahim [29], Sharma [30], Ibrahim et al. [31], and Ibrahim et al. [32] reported studies on viscous dissipation and heat source factors.

The freezing of soul around the heat exchanger coils the melting of soil and permafrost, thawing of frozen grounds, the preparation of semiconductor material, the freeze treatment sewage and casting and welding of melting phenomenon [33]. For the first time the melting heat phenomenon of ice slab due to hot air stream was analyzed by Robert [34].

The thermal-diffusion (Soret) effect, for instance, has been utilized for isotope separation, and in mixture between gases with very light molecular weight (H2, He) and of medium molecular weight (N2, air), the diffusion-thermo (Dufour) effect was found to be of a considerable magnitude such that it cannot be ignored (Eckert and Drake [35]). Subhakar et al. [36] proposed the combined effects of Soret and Dufour effects on MHD flow over a moving non-isothermal vertical plate in presence of heat source. Soret and Dufour effects on MHD convection flow of nanofluids over a vertical non-linear stretching/shrinking sheet with radiation was carried out by Pal et al. [37].

To the authors' knowledge, no investigation have this far been done with regard to study the flow and heat transfer distinctiveness of Williamson nanofluid past over a nonlinear variable thicked surface with magnetohydrodynamics and melting heat transfer effects. So the main aim of the present investigation is to extend the effort of reference Hayat et al.

[14] in three directions: (1) to consider thermal radiation (2) to consider the heat source (3) to consider the viscous dissipation effects.

Mathematical formulation

We assume the laminar flow of Williamson nanofluid towards a nonlinearly stretched sheet with variable thickness. The *x*-axis is along the sheet while y-axis is normal to x-axis. A non –uniform magnetic field $B(x) = B_0 \left(X + b \right)^{\frac{n-1}{2}}$ is applied normal to the flow direction (see Fig.1). Heat transfer analysis is carried in presence of melting heat transfer. Flow analysis further contains Brownian motion and thermophoresis effects. Moreover surface is assumed at $y = \delta \left(x + b \right)^{\frac{1-n}{2}}$ (where δ s small so that surface is sufficiently thin).The constitutive equations of the Williamson fluid model are given in Nadeem et al.[2]:

$$divV=0, \tag{1}$$

$$\rho \frac{dv}{dt} = div\ S + J \times B(x), \tag{2}$$

$$S = -\rho I + \tau, \tag{3}$$

$$V = \left[u\left(x, y\right), v\left(x, y\right), 0 \right], \tag{4}$$

$$J = \sigma \left(V \times B(x) \right), \tag{5}$$

$$B(x) = \left[0, B(x), 0 \right], \tag{6}$$

$$\tau = \left(\mu_\infty + \frac{\mu_0 - \mu_\infty}{1 - \Gamma \dot{\gamma}} \right) A_1, \tag{7}$$

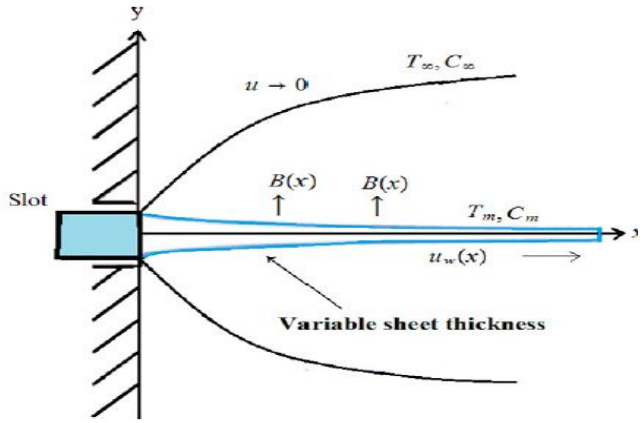

Fig. 1 Physical model.

Where $\boldsymbol{V}$ is the velocity vector, $\boldsymbol{S}$ is the Cauchy stress tensor, $\boldsymbol{J}$ rep-resents the current density, $B(x) = B_0\left(X + b\right)^{\frac{n-1}{2}}$ the non-uniform magnetic field, σ the electrical conductivity, B_0 the applied magnetic field, $\frac{d}{dt}$ represents the material time derivative, p is the pressure, $\boldsymbol{I}$ the identity tensor, τ the extra stress tensor, $\left(\mu_0, \mu_\infty\right)$ the limiting viscosities at zero and infinite shear rates, $\Gamma > 0$ the time constant, A_1 the first Rivlin-Erickson tensor and γ is define as

$$\gamma = \sqrt{\frac{1}{2}\sum_i\sum_j \gamma_{ij}\gamma j_{ji}} = \sqrt{\frac{\pi}{2}}.\pi = trace\left(A_1^2\right), \tag{8}$$

$$\gamma = \sqrt{\left[\left(\frac{\partial u}{\partial x}\right)^2 + \frac{1}{2}\left(\frac{\partial u}{\partial y} + \frac{\partial v}{\partial x}\right)^2 + \left(\frac{\partial v}{\partial y}\right)^2\right]}, \tag{9}$$

Where π is the second invariant strain tensor. Here we have only considered the case for which $\mu_\infty = 0$ and $\Gamma\gamma < 1$.Then we obtain

$$\tau = \left(\frac{\mu_0}{1-\Gamma\gamma}\right)A_1, \tag{10}$$

By employing binomial expansion we get

$$\tau = \mu_0\left(1+\Gamma\gamma\right)A_1, \tag{11}$$

Making use of Eqs.(3) and (11) in Eqs.(1) and (2) and adopting the procedure in Ref. [38] and then employing the boundary layer assumptions Ref. [39] we have the following governing equations:

$$\frac{\partial u}{\partial x} + \frac{\partial v}{\partial y} = 0, \tag{12}$$

$$u\frac{\partial u}{\partial x} + v\frac{\partial v}{\partial y} = v\frac{\partial^2 u}{\partial y^2} + \sqrt{2}v\Gamma\left(\frac{\partial u}{\partial y}\right)\frac{\partial^2 u}{\partial y^2} - \frac{\sigma B^2(x)}{\rho f}u, \tag{13}$$

$$u\frac{\partial T}{\partial x} + v\frac{\partial T}{\partial y} = \alpha_f\frac{\partial^2 T}{\partial y^2} + \tau\left(D_B\frac{\partial c}{\partial y}\frac{\partial T}{\partial y} + \frac{D_T}{T\infty}\left(\frac{\partial T}{\partial y}\right)^2\right) - \frac{1}{\left(\rho c\right)_f}\frac{\partial q_r}{\partial y} + \frac{\upsilon}{c_p}\left(\frac{\partial u}{\partial y}\right)^2 + \frac{Q'}{\left(\rho c\right)_f}\left(T - T_\infty\right) \tag{14}$$

$$u\frac{\partial C}{\partial x} + v\frac{\partial C}{\partial y} = D_B\frac{\partial^2 C}{\partial y^2} + \frac{D_T}{T\infty}\frac{\partial^2 T}{\partial y^2}, \tag{15}$$

With the subjected conditions

$$u = u_w(x) = a(x+b)^n, T = T_m, C = C_m \quad \text{at} \quad y = \delta(x+b)^{\frac{1-n}{2}},$$

$$u \to 0, T \to T_\infty, C \to C_\infty, \quad \text{as} \quad y \to \infty, \tag{16}$$

$$k\left(\frac{\partial T}{\partial y}\right)\Big|_{\delta(x+b)^{\frac{1-n}{2}}} = \rho_f\left[\lambda_1 + C_s(T_m - T_0)\right]v\left(x, y = \delta(x+b)^{\frac{1-n}{2}}\right),$$

Where *(u,v)* are the velocity components parallel to *x* and *y* directions respectively, Γ the material parameter of Williamson fluid, ν the kinematic viscosity, ρ_f the density of base fluid, *T* the fluid temperature, $\tau = \frac{(\rho C)_p}{(\rho C)_f}$ the heat capacity ratio, $(\rho C)_f$ the heat capacity of fluid , $(\rho C)_p$ the effective heat capacity of nanoparticles, D_B the Brownian diffusion coefficient, D_T the thermophoretic diffusion coefficient, $\alpha_f = \frac{k}{(\rho C)_f}$ the thermal diffusivity of fluid, *k* the thermal conductivity of fluid, $u_w(x)$ the stretching velocity, λ_1 the latent heat, C_s the heat capacity of solid, T_m the melting surface temperature, T_0 the temperature of sold, c_p is the specific heat at constant pressure, q_r is the radiative heat flux, Q' is the heat generation coefficient *(a, b)* the dimensional constants and *n* the power index.

Using Rosseland approximation for radiation, the radiative heat flux is simplified as,

$$q_r = -\frac{4\sigma^*}{3k^*}\frac{\partial T^4}{\partial y} \tag{17}$$

where σ^* is the Stephen Boltzmann constant and k^* is the mean absorption coefficient.

It should be noted that by using the Rosseland approximation, the present analysis is limited to optically thick fluids. If the temperature differences within the flow are sufficiently small, then equation (17) can be linearized by expanding T^4 into the Taylor series about T_∞, which after neglecting higher order terms takes the form

$$T^4 \cong 4T_\infty^3 T - 3T_\infty^4 \tag{18}$$

Substituting (17) and (18) in (14), we have

$$u\frac{\partial T}{\partial x} + v\frac{\partial T}{\partial y} = \alpha_m\frac{\partial^2 T}{\partial y^2} + \tau\left[D_B\left(\frac{\partial C}{\partial y}\frac{\partial T}{\partial y}\right) + \frac{D_T}{T_\infty}\left(\frac{\partial T}{\partial y}\right)^2\right] + \frac{16\sigma^*}{3k^*}\frac{T_\infty^3}{(\rho c)_f}\frac{\partial^2 T}{\partial y^2} + \frac{\upsilon}{c}\left(\frac{\partial u}{\partial y}\right)^2 + \frac{Q'}{(\rho c)_f}(T - T_\infty) \tag{19}$$

The governing equations can be reduced to ordinary differential equations, using the following similarity transformation,

$$\psi=\sqrt{\left(\frac{2}{n+1}\right)a\nu\left(x+b\right)^{n+1}F(\eta)},\ \eta=y\sqrt{\left(\frac{n+1}{2}\right)\left(\frac{a}{\nu}\right)}(x+b)^{n-1},\ u=a(x+b)^{n}F'(\eta),$$

$$v=-\sqrt{\left(\frac{n+1}{2}\right)a\nu\left(x+b\right)^{n+1}\left(f(\eta)+\eta\frac{n-1}{n+1}F\left(\eta\right)\right)},\ \theta\left(\eta\right)=\frac{T-T_m}{T_\infty-T_m},\ \phi\left(\eta\right)=\frac{C-C_m}{C_\infty-C_m},\qquad(20)$$

Eq.(12)is trivially satisfied and other equations are reduced to

$$F'''-\frac{2n}{n+1}F'^{2}+FF''+\lambda\sqrt{\frac{n+1}{2}}F''F'''-Ha^{2}+\frac{2}{n+1}F=0,\qquad(21)$$

$$F'''\left(\zeta\right)-\frac{2n}{n+1}F'^{2}\left(\zeta\right)+F\left(\zeta\right)F''\left(\zeta\right)+\lambda\sqrt{\frac{n+1}{2}}F''\left(\zeta\right)F'''\left(\zeta\right)-Ha^{2}\frac{2}{n+1}F'\left(\zeta\right)=0\qquad(22)$$

$$\phi''\left(\zeta\right)+ScF\left(\zeta\right)\phi'\left(\zeta\right)+\frac{Nt}{Nb}\phi''\left(\zeta\right)=0,\qquad(23)$$

$$F(\alpha)=1,M\theta'(\alpha)+\left(F(\alpha)+\alpha\frac{n-1}{n+1}\right)=0,\quad\theta\left(\alpha\right)=0,\phi\left(\alpha\right)=0,$$

$$F\left(\infty\right)=0,\ \theta\left(\infty\right)=1,\ \phi\left(\infty\right)=1,\qquad(24)$$

where $\alpha=\delta\sqrt{\frac{n+1}{2}\frac{a}{\nu}}$ is the wall thickness parameter. Eqs.(21)-(23) can be transformed into the system of

dimensionless expressions by utilizing

$$F\left(\zeta\right)=f\left(\zeta-\alpha\right)=f\left(\xi\right),\quad\theta\left(\zeta\right)=\theta\left(\zeta-\alpha\right)=\theta\left(\xi\right),\ \text{and}\ \phi\left(\zeta\right)=\phi\left(\zeta-\alpha\right)=\phi\left(\xi\right).$$

$$f'''\left(\zeta\right)-\frac{2n}{n+1}f'^{2}\left(\zeta\right)+f\left(\zeta\right)f''\left(\zeta\right)+\lambda\sqrt{\frac{n+1}{2}}f''\left(\zeta\right)f'''\left(\zeta\right)-Ha^{2}\frac{2}{n+1}f'\left(\zeta\right)=0\qquad(25)$$

$$\left(1+\frac{4}{3}R\right)\theta''\left(\zeta\right)+\Pr f\left(\zeta\right)\theta'\left(\zeta\right)+\Pr Nb\theta'\left(\zeta\right)\phi'\left(\zeta\right)+\Pr Nt\left(\theta'\left(\zeta\right)\right)^{2}+\Pr Ecf''^{2}\left(\zeta\right)+\Pr Q\theta\left(\zeta\right)=0$$

(26)

$$\phi''\left(\zeta\right)+Sc\phi'\left(\zeta\right)+\frac{Nt}{Nb}\theta''\left(\zeta\right)=0\qquad(27)$$

$$f'(0)=1,M\theta'\left(0\right)+\Pr\left(f\left(0\right)+\alpha\frac{n-1}{n+1}\right)=0,\ \theta\left(0\right)=0,\phi\left(0\right)=0,$$

$$f'\left(\infty\right)=0,\ \theta\left(\infty\right)=1,\ \phi\left(\infty\right)=1.\qquad(28)$$

Here Weissenberg number λ, thermophoretic parameter *Nt*, Prandtl number *Pr*, Brownian motion parameter *Nb*, Schmidt number *Sc*, Hartman number *Ha* and melting heat transfer parameter *M*, heat source parameter *Q*, radiation parameter *R* and viscous dissipation factor *Ec* are defined as follows:

$$\lambda=\Gamma\left(\frac{a^3(x+b)^{3n-1}}{\nu}\right)^{\frac{1}{2}},\ M=\frac{(C_p)_f(T_\infty-T_m)}{\lambda_1+C_f(T_m-T_0)},\ Nt=\frac{\tau D_T(T_\infty-T_m)}{T_\infty\nu},\ Nb=\frac{\tau D_T(C_\infty-C_m)}{\nu},\ Ha^2=\frac{\sigma B^2(x)}{\rho_f a(x+b)^{n-1}},$$

$$Sc=\frac{\nu}{D_B},\ \Pr=\frac{\nu}{\alpha_f},\ Q=\frac{Q'}{a\rho c_p},\ R=\frac{4\sigma^* T_\infty^3}{kk^*},\ Ec=\frac{U_w^2}{c_p(T_\infty-T_m)} \qquad (29)$$

It should be noted that the results for viscous fluid can be recovered by putting $\lambda=0$.

The Skin friction coefficient, local Nusselt and Sherwood numbers are

$$C_f=\frac{T_w}{\rho u_w{}^2},\ Nu=\frac{(x+b)q_w}{k(T_\infty-T_m)},\ Sh=\frac{(x+b)q_m}{k(C_\infty-C_m)}, \qquad (30)$$

In which the surface shear stress (T_w), surface heat flux (q_w) and surface mass flux (q_m) satisy the below mentioned relations:

$$\tau_w=\mu\left(\frac{\partial u}{\partial y}+\frac{\Gamma}{\sqrt{2}}\left(\frac{\partial u}{\partial y}\right)^2\right)\Bigg|_{y=b(x+b)^{\frac{1-n}{2}}},\ q_w=-k\left(\frac{\partial T}{\partial y}\right)\Bigg|_{y=\delta(x+b)^{\frac{1-n}{2}}},\ q_m=-D_B\left(\frac{\partial C}{\partial y}\right)\Bigg|_{y=\delta(x+b)^{\frac{1-n}{2}}} \qquad (31)$$

Substituting Eq-(31) in Eq.(30) the skin friction coefficient, local Nusselt and Sherwood numbers can be put into the forms:

$$\sqrt{\mathrm{Re}_x}C_f=\left(\sqrt{\frac{n+1}{2}}f''(0)+\lambda\frac{n+1}{4}(f''(0))^2\right),\ \frac{Nu}{\sqrt{\mathrm{Re}_x}}=-\sqrt{\frac{n+1}{2}}\theta'(0),$$

$$\frac{Sh}{\sqrt{\mathrm{Re}_x}}=-\sqrt{\frac{n+1}{2}}\phi'(0), \qquad (32)$$

$$\mathrm{Re}_x=\frac{a}{\nu}(x+b)^{n+1}=\frac{u_w}{\nu}(x+b), \qquad (33)$$

Where Re_x is the local Reynolds number and ν the kinematic viscosity.

Description of Results: The reduced Eqs. (25)–(27) are nonlinear and coupled, and thus their exact analytical solutions are not possible. They can be solved numerically using Runge–Kutta– Fehlberg fourth fifth order method for different

values of governing parameters. The effects of the emerging parameters on the dimensionless velocity, temperature, skin-friction, the rates of heat and mass transfer are investigated. The step size and convergence criteria were chosen to be 0.001 and 10-6, respectively. The asymptotic boundary conditions in Eq. (9) were approximated by using a value of 8 for ζ as follows: $\zeta_{Max} = 8$. This ensures that all numerical solutions approached the asymptotic values correctly.

In order to get the group of equations (25)-(27) based on the boundary conditions (28) are resolved via shooting approximation. Further, to judge the accuracy of reliable analysis, comparison with available results of Hayat et al. [14] corresponding to coefficients (Table1) and found in good agreement. For numerical results, we considered the values to the non-dimensional parameters as *Ha = 0.5, n = 1.5,* $\lambda = 0.2$, *Pr = 0.71,* α *=0.2, M = 0.4, Ec = 0.1, Q = 0.1, R = 1.0, Nt = 0.2, Nb = 0.4, Sc = 1.2.*

Table-1. Comparison of $-f''(0)$**,** $-\theta'(0)$ **and** $-\phi'(0)$ **for different values of** ζ **when *n = 1.5, Ha =*** $\alpha = Nt = \lambda$ ***=0.2, Pr = 1.0, Sc = 1.2, Nb = 0.4* and *M = 0.4*.**

	Hayat et al. [14]			Present		
ζ	$-f''(0)$	$-\theta'(0)$	$-\phi'(0)$	$-f''(0)$	$-\theta'(0)$	$-\phi'(0)$
1	0.8612	0.9192	0.9269	0.861012	0.919185	0.926871
5	0.9041	0.7239	0.5910	0.904043	0.723854	0.590945
10	0.9347	0.6134	0.2937	0.934618	0.613389	0.293639
15	0.9509	0.5540	0.1952	0.951024	0.553901	0.195178

These values are kept as common for the complete study unless otherwise they showed in the plots.

Figs. 2- 4 depict the variation of $f'(\zeta), \theta(\zeta)$ and $\phi(\zeta)$ for various values of Ha. The velocity, temperature and concentration distributions decreased when the Hartman number increases. The fluid velocity for hydrodynamic case is stronger in comparison to hydromagnetic situation. The Lorentz force appeared in magnetic parameter becomes stronger with an increase in *Ha*. In fact the stronger Lorentz force decays the velocity. Characteristics of power - law index parameter n on velocity, temperature and concentration are portrayed in Figs. 5 -7. It is clear that increasing the power law index n rises the fluid velocity. The opposite behavior is found in both temperature and concentration. Generally, rising values of n reduce the non-Newtonian behavior of the flow, and this leads to enhance the momentum boundary

layer. The effect of the melting parameter M can be understood from the variation in the velocity, temperature and concentration components with the similarity independent variable ζ as displayed in Figs. 8 – 10. It is observed from Fig. 8 that the fluid velocity enhances with the increase in the melting parameter M within the boundary layer region. But the reverse effect occurs in temperature and concentration distributions. Fig. 11 is designed to analyze the variation on velocity distribution under the action of Weissenberg number (λ). it is observed that velocity increases for greater value of Weissenberg number. Physically Weissenberg number is the ratio of relaxation time of the fluid and a specific process time. It increases the thickness of the fluid due to which the velocity profile decreases. Fig. 12 Presents the effect of Pr on temperature profiles. In the presence of melting parameter, an increase in Prandtl number increases the temperature profiles. Prandtl number is the ratio of momentum diffusivity to thermal diffusivity. Higher Prandtl number corresponds to lower thermal diffusivity. Hence less heat is transferred from heated fluid to the melting surface and as a result the temperature distribution remains higher. The impact of the thermal radiation parameter *R* in the presence of the Hartman number and melting parameter on the temperature profiles of an electrically conducting fluid is presented in Fig. 13. From Fig. 13 it can be seen that the temperature distribution decreases uniformly with increasing thermal radiation parameter. The behavior of fluid temperature by the influence of heat source (*Q*), viscous dissipation (*Ec*), thermphoresis (*Nt*) and Brownian motion (*Nb*) parameters are displayed in Figs. 14- 17. It is seen that *Q, Ec, Nt* and *Nb* increase the fluid temperature. Fig. 18 portrays the effect of wall thickness parameter (α) on the temperature profile. It is seen that the temperature profile and thermal boundary layer thickness are reducing function of wall thickness parameter. Small quantity of heat is transferred from sheet to the fluid when wall thickness parameter is enhanced. Due to this cause the temperature profile reduces. Figs. 19 -21 illustrate the effects of Schmidt number, thermophoresis and Brownian motion parameters on the concentration profiles. It is clear that the concentration boundary layer thickness increases as both Sc and Nb increase, whereas an increase in the Nt has the opposite effect. The numerical comparisons of, $f''(0)+\frac{\lambda}{2}\left(f''(0)\right)^2, -\theta'(0)$ and $-\phi'(0)$ for the different values of *M,* λ *,n, M, Pr, R, Q, Ec, Nb, Nt,* and *Sc* are shown in table 2 -4. The variation in skin-friction coefficient, Nusselt number and Sherwood number for various parameters are investigated through tables 2 - 4. The behavior of theses physical parameters is self evident from tables 2 -4 and hence they are not discussed any further to keep brevity.

Table-2. Values skin-friction factor, wall temperature gradient and wall nanoparticle volume fraction gradient for different values of the parameters.

Ha	*n*	λ	*M*	C_f	*Nu*	*Sh*
0.5	1.5	0.2	0.4	1.355722	1.224132	0.832704
1.0				1.505561	1.182498	0.807792
2.0				1.758866	1.111875	0.762446
	2.0			1.417994	1.206899	0.822507
	3.0			1.638668	1.145339	0.784514
		0.1		1.393758	1.234585	0.839557
		0.3		1.311979	1.211385	0.823985
			1.0	1.313315	0.936316	0.610993
			2.0	1.265734	0.791154	0.215864

Table-3. Values skin-friction factor, wall temperature gradient and wall nanoparticle volume fraction gradient for different values of the parameters.

Pr	*R*	*Q*	*Ec*	C_f	*Nu*	*Sh*
0.71	1.0	0.1	0.1	1.231462	1.124132	0.732704
1.0				1.255723	0.461755	0.807618
2.0				1.249355	0.760134	0.850689
	2.0			1.257957	1.092028	0.769501
	3.0			1.260568	1.054548	0.813065
		0.5		1.241239	1.334387	0.518929
		1.0		1.216046	1.706396	0.214694
			0.5	1.251988	1.178165	0.658205
			1.0	1.247389	1.244853	0.568141

Table-4. Values skin-friction factor, wall temperature gradient and wall nanoparticle volume fraction gradient for different values of the parameters.

Nb	*Nt*	*Sc*	α	C_f	*Nu*	*Sh*
0.2	0.4	1.2	0.2	1.255727	1.124139	0.732704
0.3				1.234018	1.440065	0.726717
0.5				1.213999	1.738353	0.584668
	0.3			1.239396	1.361258	0.643791
	0.5			1.220633	1.638234	2.620587
		20.0		1.253685	1.153597	0.969584
		30.0		1.252847	1.165789	0.998209
			0.1	1.256267	1.116358	0.675045
			0.2	1.256823	1.108365	0.615484

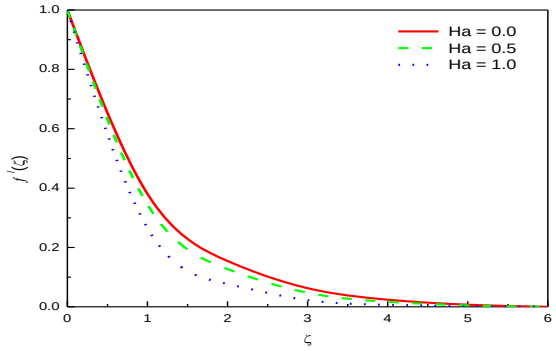

Fig2. Behavior of *Ha* on $f'(\zeta)$

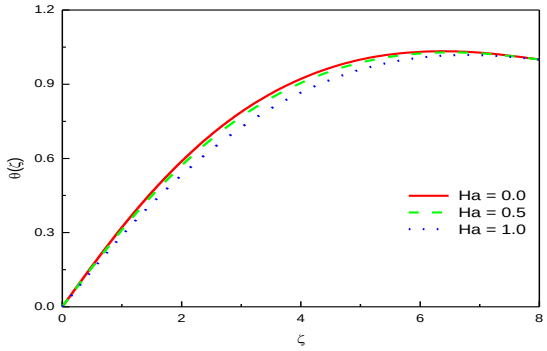

Fig3. Behavior of *Ha* on $\theta(\zeta)$

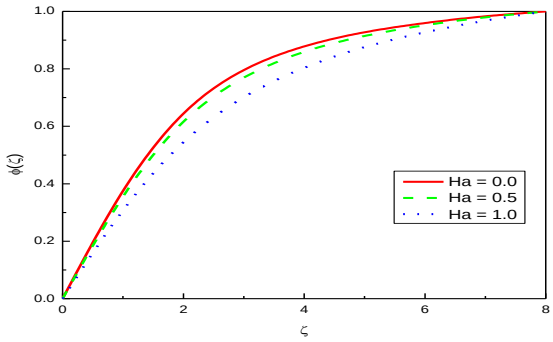

Fig4. Behavior of *Ha* on $\phi(\zeta)$

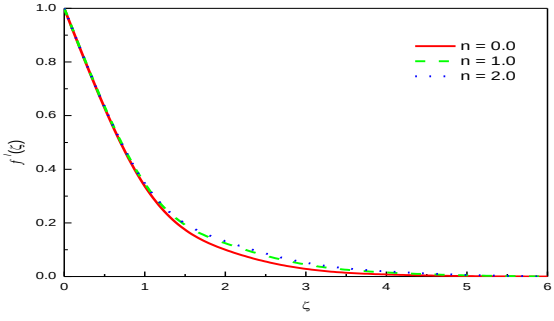

Fig. 5. Behavior of *n* on $f'(\zeta)$

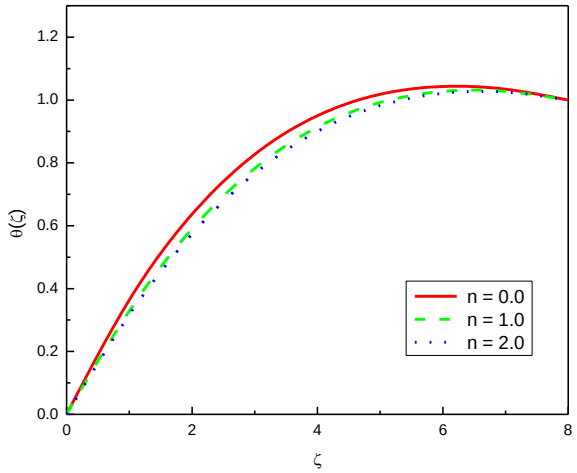

Fig. 6 Behavior of n on $\theta(\zeta)$

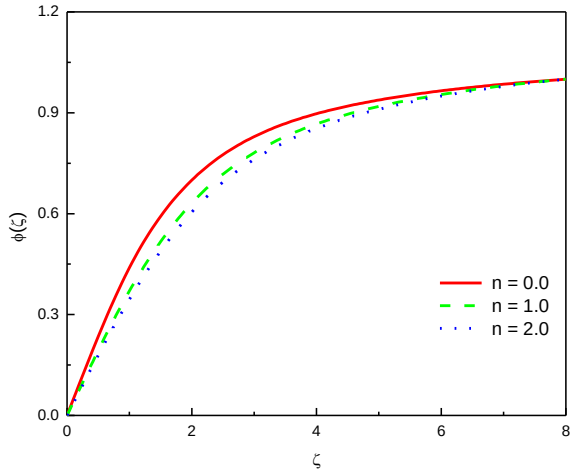

Fig. 7. Behavior of n on $\phi(\zeta)$

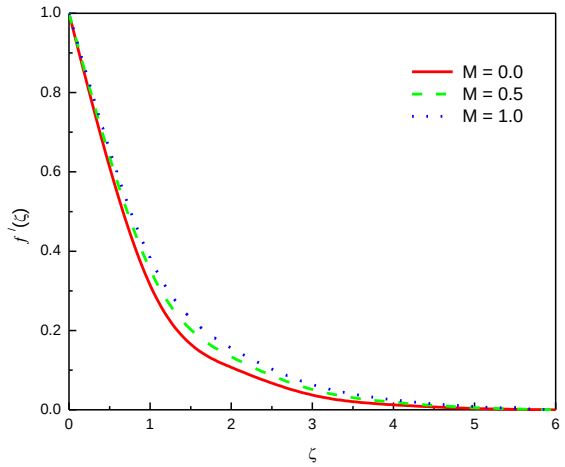

Fig. 8. Behavior of M on $f'(\zeta)$

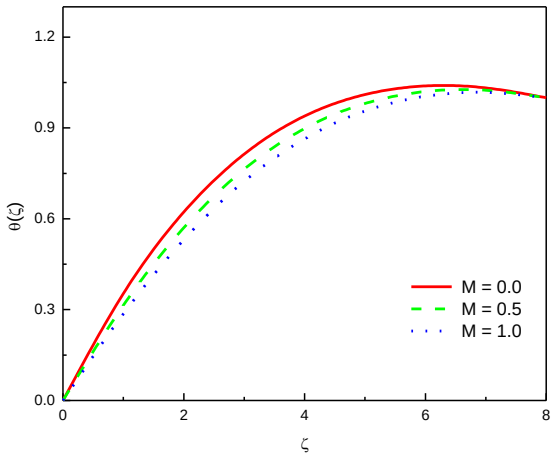

Fig. 9. Behavior of M on $\theta(\zeta)$

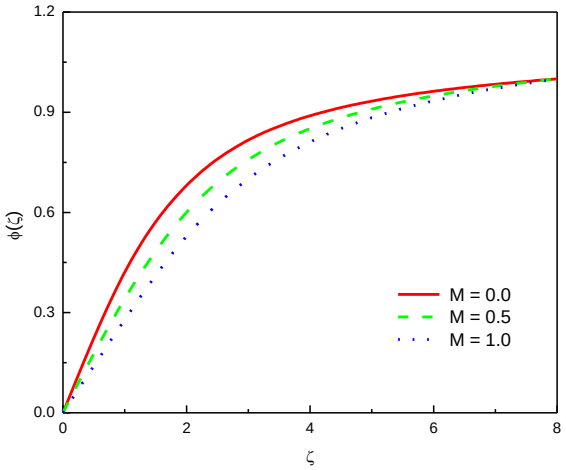

Fig. 10. Behavior of M on $\phi(\zeta)$

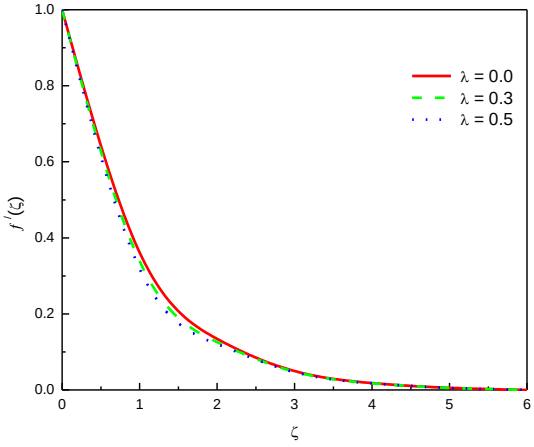

Fig. 11 . Behavior of λ on $f'(\zeta)$

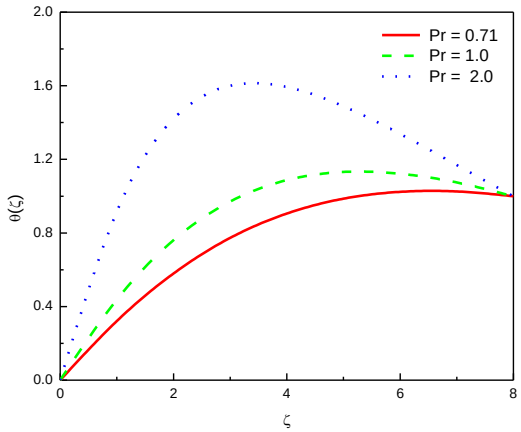

Fig. 12 Behavior of *Pr* on $\theta(\zeta)$

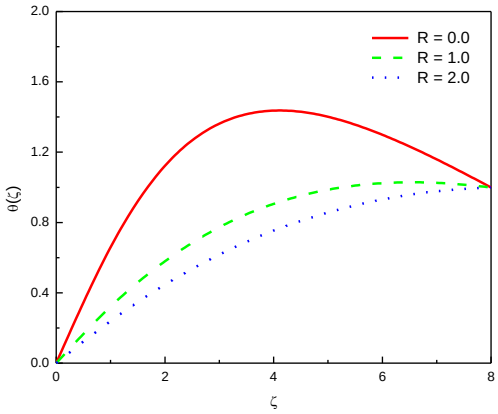

Fig. 13. Behavior of *R* on $\theta(\zeta)$

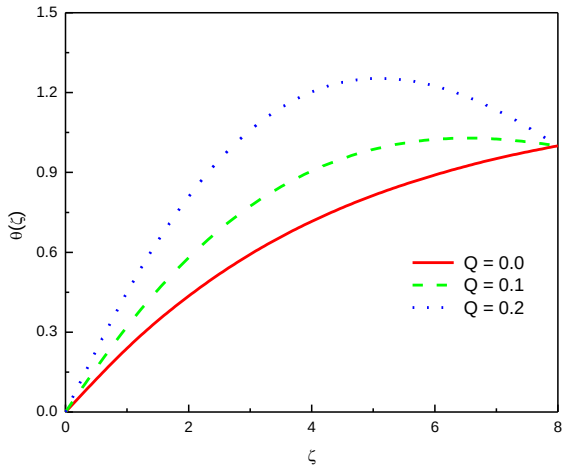

Fig 14. Behavior of *Q* on $\theta(\zeta)$

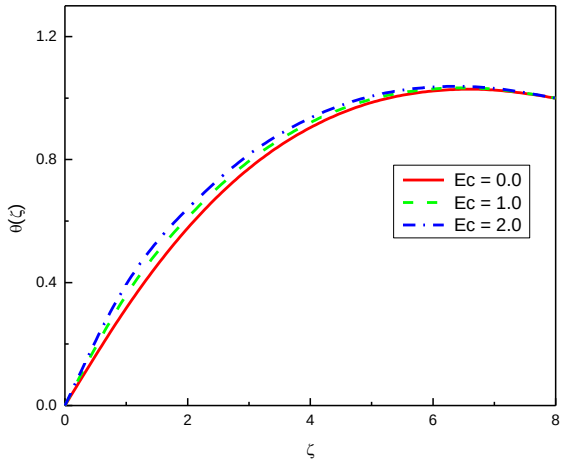

Fig. 15. Behavior of *Ec* on $\theta(\zeta)$

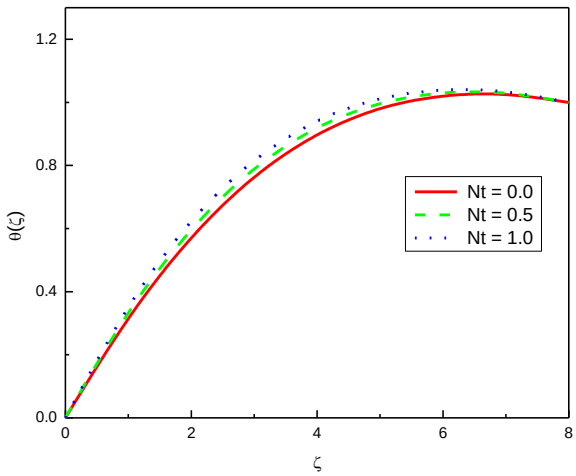

Fig. 16. Behavior of *Nt* on $\theta(\zeta)$

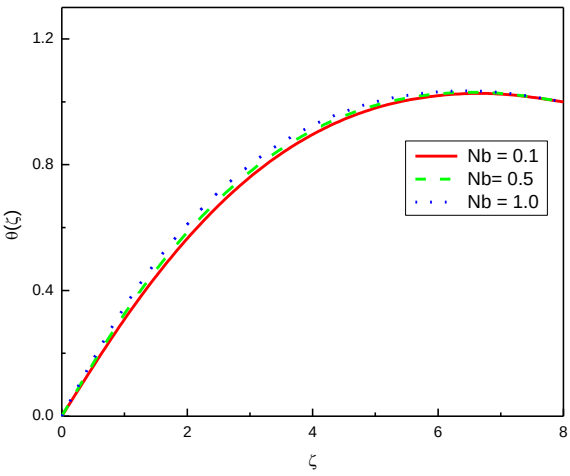

Fig. 17. Behavior of *Nb* on $\theta(\zeta)$

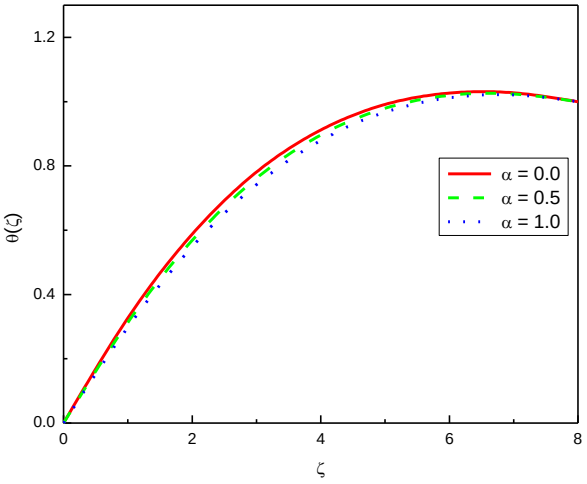

Fig. 18. Behavior of α on $\theta(\zeta)$

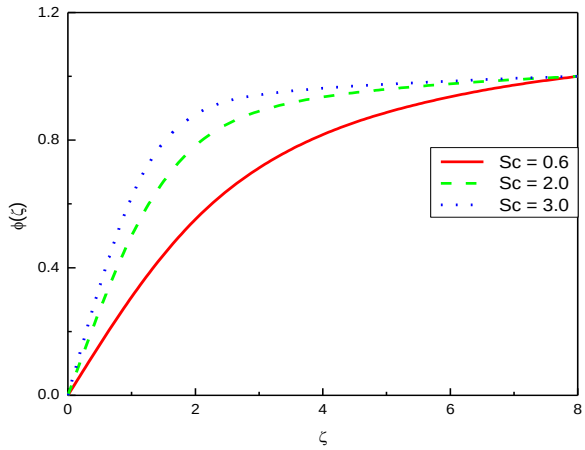

Fig. 19. Behavior of *Sc* on $\phi(\zeta)$

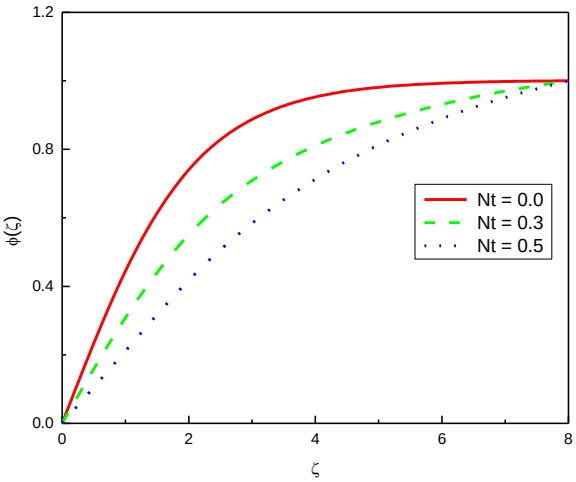

Fig. 20. Behavior of *Nt* on $\phi(\zeta)$

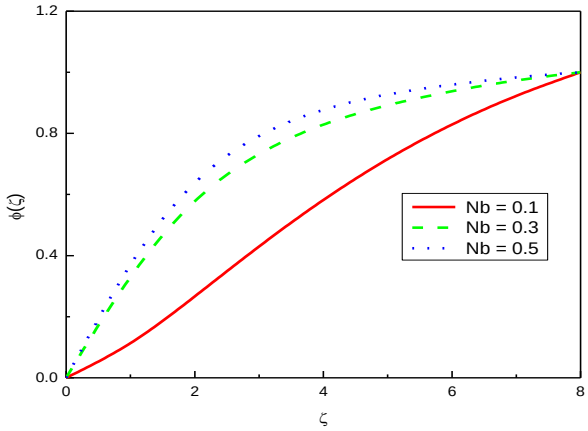

Fig. 21. Behavior of *Nb* on $\phi(\zeta)$

Conclusion

In this paper, we studied the Melting heat transfer in the flow of MHD Williamson nanofluid over a variable thicked stretching sheet in presence of thermal radiation, heat source and viscous dissipation. The salient features of this investigation are explained below.

- Increasing the radiation factor and Hartman number leads to deceleration of the temperature but the effect is reverse for the Prandtl number.
- Characteristics of Weissenberg and Hartman numbers on velocity distribution are opposite to that of melting parameter and power-law factor.

- Both local Nusselt number and local Sherwood number increase with Schmidt number.
- The heat source parameter and Eckert number increases the heat transfer rate, but decreases the mass transfer rate.
- The skin-friction factor, Nusselt number and Sherwood number decreases with increase in the melting parameter, whereas the effect is opposite for Prandtl number.

References

1. S.U.S. Choi, 1995,Vol 66,pp.99–105.
2. J. A. Eastman, S. U. S. Choi, S. Li, W. Yu, and L. J. Thompson, 2001,Vol 78, pp.718–720.
3. H. Q. Xie, H. Lee, W. Youn, and M. Choi, 2003,Vol 94, pp. 4967–4971.
4. S. Jana, A. Salehi-Khojin, and W. H. Zhong, 2007, Vol .462,pp.45–55.
5. R.V. Williamson, 1992,Vol. 21,pp.1108–1111.
6. S. Nadeem, S.T. Hussain, C. Lee, 2013, Vol .30,pp. 619–625.
7. Crane, L.J, 1970,Vol .21,pp. 645-647.
8. C.Y.Wang, 1984, Vol. 27,pp. 1915-1917.
9. H.I.Andersson, 1992, Vol .95, pp.227-230.
10. P.S.Gupta, and A.S.Gupta, 1977, vol .55, pp.744-746.
11. K Vajravelu, 2001, Vol .124, pp. 281-288.
12. A. Raptis, and C. Perdikis, 2006, Vol .41, pp.527-529.
13. R. Cortell, 2007, Vol.184,pp. 864-873.
14. T.Hayat ., G Bashir., M. Waqas., and A. Alsaedi, 2016, Vol .223, pp. 836–844.
15. F Mabood., S.M Ibrahim., G.Lorenzini., and E. Lorenzini, 2017, Vol. 35(1), pp. 196-204.
16. M. Farooq, M.I. Khan, M. Waqas, T. Hayat, A. Alsaedi, M.I. Khan, 2016, Vol.221 pp.1097–1103.
17. S.M.Ibrahim ,N.B. Reddy, 2012,Vol. 8(8), pp. 1-21.
18. S. M. Ibrahim, F. Mabood, K. Suneetha, and G. Lorenzini, 2017, Vol. 26(2), pp. 234–255.
19. R.G.A. Rahman, M.M. Khadar, A.M. Megahed, 2013, Vol. 22 , 030202.

20. C. S. K. Raju., P. Sanjeevi., M. C. Raju., S. M. Ibrahim · G. Lorenzini., and E. Lorenzini, DOI 10.1007/s00161-017-0580-z.
21. Ch Sumalatha and B Shankar, 2015, Vol.5, pp.257-265.
22. M.M. Nandeppanavar, K. Vajravelu, and M. Subhas Abel, 2011,Vol.16, pp. 3578-3590.
23. K.Bhattacharyya, K. 2011, Vol. 5, pp.376- 384.
24. H Dessie and N Kishan, 2014,Vol. 5 (3), pp. 967 – 977.
25. M.R Krishnamurthy., B.C Prasannakumara., B.J Gireesha, and R.S.R Gorla, 2015, Vol. 2: 1050973.
26. P Sreenivasulu., T.Poornima., and N Bhaskar Reddy, 2015 March 26-28, 2015, Gauhati University, Guwahati, Assam, India.
27. A.J. Chamkha and A.M Aly, 198: Vol.3, pp.425 — 441.
28. M.S.Abel, and G.Begum, 2008, Vol.195, pp. 1503–1523.
29. W. Ibrahim, 2015,Vol. 4, pp. 157-166.
30. R. Sharma, 2012,Vol. 219, pp. 976-987.
31. S. M. Ibrahim, P. V. Kumar, G. Lorenzini, E. Lorenzini, and F. Mabood, 2017, Vol. 26(2), pp. 256–271.
32. S.M. Ibrahim, G. Lorenzini, P. Vijaya Kumar, C.S.K. Raju, 2017, Vol.111, pp. 346–355.
33. R.G.A. Rahman, M.M. Khadar, A.M. Megahed, B 2013, Vol.22, pp.030202.
34. L. Robert, 1958, Vol. 4,pp. 505–528.
35. E.R.G. Eckert, and R.M. Drake, Analysis of Heat and Mass Transfer. McGraw-Hill Book Co., New York, 1972.
36. M.J Subhakar., K Gangadhar., and N Bhaskar Reddy, 2012, Vol. 3 (5), pp.3165-3184.
37. D Pal., G Mandal, and K Vajravalu, 2016, Vol. 287 (288), pp. 184- 200.
38. J. Harris, Rheology and Non-Newtonian Flow, Longman, London, 1977.
39. H. Schichting, Boundary Layer Theory, 6th ed. ed., McGraw-Hill, New York, 1964.

Corresponding Author:

K. Suneetha[*],

Email: s.sunibabu@gmail.com